Spin-Echo Resolved Grazing Incidence Scattering (SERGIS) at Pulsed and CW Neutron Sources

Rana Ashkar[1], P Stonaha[1], A Washington[1], V R Shah[1], M R Fitzsimmons[2], B Maranville[3], C F Majkrzak[3], W T Lee[4], Roger Pynn[1, 4]

[1]Indiana University Cyclotron Facility, Bloomington, IN 47408, USA
[2]Los Alamos Neutron Scattering Center, Los Alamos, NM 87545, USA
[3]NIST Center for Neutron Research, Gaithersburg, MD 20899, USA
[4]Neutron Science Directorate, Oak Ridge National Lab, Oak Ridge, TN 37831, USA

e-mail: rashkar@indiana.edu

Abstract. We have used SERGIS to probe the surface structure of a silicon diffraction grating of period 140 nm. Experiments were performed at: the Los Alamos Neutron Science Center (LANSCE) pulsed neutron source and the National Institute of Standards and Technology (NIST) continuous wave (CW) reactor neutron source. Although both sets of data show peaks of the spin echo polarization at integer multiples of the grating period, as expected, the results differ in detail. We have developed a dynamical theory, based on a Bloch wave expansion, to describe neutron diffraction from a grating. The theory explains the differences between the two sets of data without any adjustable parameters.

1. Introduction
Physical constraints, such as grooves of a diffraction grating or steps on vicinal surfaces, have been recently used to direct the self-assembly of macromolecules [1, 2]. Neutron scattering is a useful technique for the characterization of the structures of such self-assembled films. Specular reflectivity [3] and a more recently developed technique, rotational SANS [4], have both been used to study the self-assembly of block copolymers (BCP) on surfaces. To study in-plane BCP ordering as a function of depth, grazing-incidence small angle scattering is needed and some experiments of this type have been performed with x-rays [5]. The SERGIS technique is being developed so that neutron scattering can be applied to such problems. As a first step in the process of developing SERGIS, we studied a bare diffraction grating of period $d = 140$ nm and groove depth $h = 65$ nm as indicated by the manufacturer and confirmed by AFM (Figure 1). Experiments on this grating were performed with the same SERGIS hardware at the LANSCE pulsed neutron source and the CW neutron source at the NIST Center for Neutron Research (NCNR). Subtle differences between the two sets of data were observed and a dynamical theory has been developed to explain the results.

2. Dynamical Theory
Neutrons scattered at grazing incidence by a periodic grating are analogous to electrons propagating in a crystal lattice in that they experience a periodic interaction potential. For neutrons the scattering potential, $V(\vec{r})$, is proportional to the scattering length density $\rho(\vec{r})$. A dynamical calculation based on a Bloch wave expansion has been used in the past [6, 7, 8] to describe the interaction of neutrons, x-rays and electrons with such periodic potentials, and we follow the same approach. The scattering

geometry is such that neutrons are incident almost parallel to the lines of the grating at a grazing angle $\theta = 0.2°$ to the surface (Figures 2, 3).
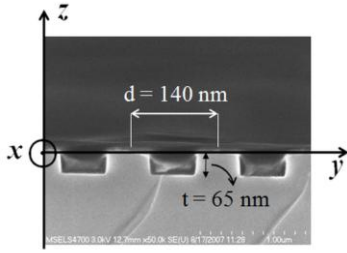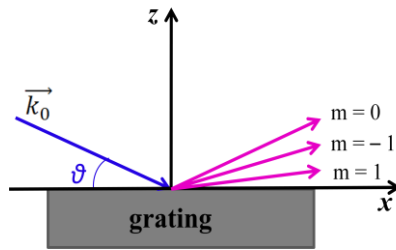
Figure 1. SEM image of the grating

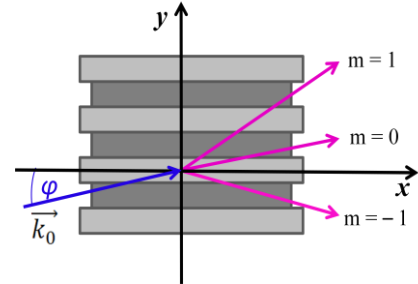**Figure 2**. Side view of the scattering geometry

Figure 3. Top view of the scattering geometry

Neutrons incident on the grating with a wavevector $\overrightarrow{k_0}$ are described by a wavefunction, ψ, that obeys the Schrödinger equation:

$$\nabla^2 \psi(\vec{r}) + \left(k_0^2 - 4\pi\rho(\vec{r}) \right) \psi(\vec{r}) = 0 \tag{1.1}$$

where $\rho(\vec{r})$ is the coherent scattering length density. We divided the grating into three layers: air with a zero scattering potential, a modulated Si-air layer with a periodic potential and a silicon substrate with a constant scattering potential. Within the modulated layer, the neutron wavefunction, ψ, can be expanded as a series of Bloch waves [6]:

$$\psi_{layer} = \sum_{n,m} [R_{1,n} e^{ik_{z,n}z} + T_{1,n} e^{-ik_{z,n}z}] b_{n,m} e^{im\left(\frac{2\pi}{d}\right)y} e^{ik_{0y}y} \tag{1.2}$$

Similar expressions of the wavefunction are used in air and the substrate:

$$\psi_{air} = [e^{-ik_{0z}z} + \sum_n R_{0,n} e^{ik'_{z,n}z} e^{in\left(\frac{2\pi}{d}\right)y}] e^{ik_{0y}y} \;;\; \psi_{sub} = \sum_n T_{2,n} e^{-ip_{z,n}z} e^{in\left(\frac{2\pi}{d}\right)y} e^{ik_{0y}y} \tag{1.3}$$

When these expressions are substituted in the Schrödinger equation, a secular equation is obtained [7]. The z-components of the wavevectors, $k_{z,n}$, are the square roots of the eigenvalues of this equation in the modulated layer and the coefficients $b_{n,m}$ are the elements of the associated eigenvectors. The wavevectors $k'_{z,n}$ and $p_{z,n}$ are the solutions of the secular equation in air and the substrate respectively. Note that both the y and z components of the diffracted wavevectors depend on the Bloch-wave index, m, as indicated in Figures 2 and 3. The amplitudes $R_{0,n}$, $R_{1,n}$, $T_{1,n}$ and $T_{2,n}$ of the Bloch waves in the different layers can be determined by equating the wavefunctions and their derivatives at the layer interfaces [8].

Using the T-matrix formalism, the scattering cross-section, $d\sigma/d\Omega$, can be expressed in terms of the matrix elements of the scattering potential operator between the state ψ and a plane wave [9]:

$$\frac{d\sigma}{d\Omega} \propto \left| < e^{i\vec{k}.\vec{r}} |V| \psi > \right|^2 \tag{1.4}$$

where $\vec{k}$ is the outgoing wavevector. The normalized SERGIS spin-echo polarization, P/P_0, is given as the cosine Fourier transform of the scattering cross-section:

$$\frac{P(y_{se})}{P_0(y_{se})} = \frac{\int_{-\infty}^{\infty} \frac{d\sigma}{d\Omega}(q_y)\cos(q_y y_{se}) dq_y}{\int_{-\infty}^{\infty} \frac{d\sigma}{d\Omega}(q_y) dq_y} \tag{1.5}$$

where P_0 is the empty-beam polarization and y_{se} is the spin-echo length (Figure 4) defined as:

$$y_{se} = (1.476 \times 10^{14} T^{-1} m^{-2}) LB\lambda^2 \cot(\alpha) \tag{1.6}$$

where B is the magnitude of the magnetic field at the interface of the triangular solenoids [10].

3. Experimental setup

The SERGIS setup consists of a neutron polarizer (placed before the upstream *π/2* flipper to the left in Figure 4), a series of magnetic flippers and triangular solenoids that control the neutron spin precession, a polarization analyzer and a detector (set in reflection geometry after the downstream *π/2* flipper to the right in Figure 4) that accepts all neutrons reflected from the surface of the grating. The polarizer polarizes the neutron beam in the |z⟩ state. The first *π/2* flipper creates an in-phase linear superposition of the |z⟩ and |-z⟩ states (corresponding to a classical spin in the y-direction). The triangular solenoids serve as birefringent media for neutrons, forcing the up and down spin states to follow different paths, as indicated in Figure 4 [10]. The separation between the paths of the two spin states as they leave the second triangular pair can be shown to be equal to the spin-echo length [10]. In our experiments, the grooves of the grating were aligned almost parallel to the x-axis ($-0.4° < \varphi < 0.4°$) thus allowing the neutron beam to probe the surface structure of the grating along the y-axis (Figure 4). The Larmor phase of each spin state depends on the time spent in each magnetic field region and consequently on the neutron trajectory. In the absence of a sample, the difference in the Larmor phase of the two spin eigenstates before the sample is cancelled in the second half of the instrument by the symmetry of the setup, and the initial neutron beam polarization is recovered as a spin echo. With a sample in place, the neutron is scattered to a different trajectory through the second half of the setup and a net Larmor phase difference between the two spin states is acquired, potentially changing the polarization of the outgoing beam. The normalized spin echo polarization is a weighted average of the cosine of the net Larmor phase difference over all detected momentum transfer i.e. the cosine Fourier transform of the scattering cross section along the y-direction, as expressed in equation (1.5).
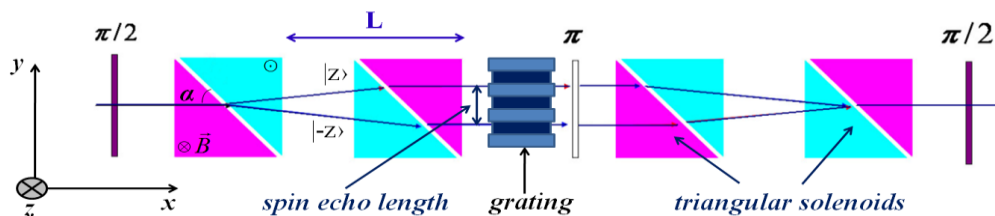

Figure 4. Top view of the experimental setup in the same configuration as Figure 3. Different shades of the triangles represent regions of opposite magnetic fields along the z-direction

4. Measurements

4.1. Data from a fixed wavelength source
Our experiment was performed at the AND/R beamline at NCNR with a beam of wavelength $\lambda = 0.5$ nm and a beam divergence in φ of 0.2° FWHM (Figure 3). The spin-echo length was scanned by varying the current in the triangular solenoids, providing a variable magnetic field strength at the interface between triangular solenoids. At 0.5 nm neutron wavelength and a current between 1A and 10A, the spin echo length ranged from ~23 nm to ~230 nm. The measured echo polarization shows peaks at integer multiples of the grating period (Figure 5).

4.2. Data from a pulsed source
At the ASTERIX beamline at LANSCE, the spin echo length varied as a function of the variable wavelength of the beam (0.4 nm < λ < 0.9 nm) at a fixed current in the solenoids. With a current of 12A we obtained a range of the spin echo length between ~90 nm and ~450 nm. Again, experimental results for the echo polarization (with a beam of 0.1° FWHM divergence in φ) show peaks at integer multiples of *d* (Figure 6).

4.3. Analytical calculations
Calculations using the dynamical formalism introduced above showed that the spin echo polarization is very sensitive to the sample alignment (i.e. the angle φ) and the beam divergence. The first order Bloch expansion (which is a three-beam approximation) gives a good account of the results we

obtained at both CW and pulsed sources as shown in Figures 5, 6. There are no adjustable parameters in the theory: all quantities (such as beam divergence, neutron wavelength, magnetic field in the triangular solenoids, etc) were set to their experimental values.
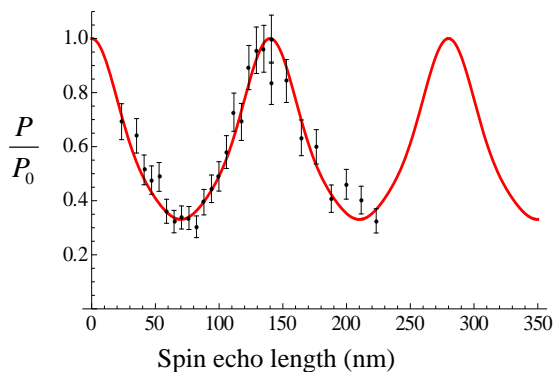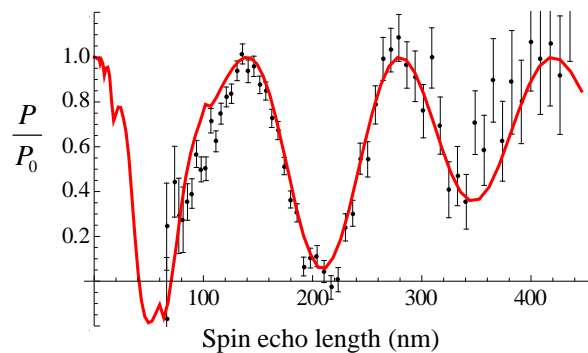

Figure 5. Plot of P/P$_0$ at NCNR

Figure 6. Plot of P/P$_0$ at LANSCE

4.4. Interpretation of results

Within a simple approximation such as the Distorted-Wave Born Approximation, the neutron scattering cross-section is proportional to the Fourier transform of the height-height correlation function of the reflecting surface, albeit modified by strongly varying optical factors [9]. Thus, we might expect the echo polarization to have a shape similar to the height-height correlation function of our grating. Since the grating profile is rectangular, the height autocorrelation function is a periodic array of isosceles triangles. Indeed, such a form with triangular peaks at integer multiples of the grating period is similar to the measured echo polarization although there are quantitative deviations from this simple form. For example, the amplitude of the oscillations is different for data at NIST and LANSCE and the second minimum in Figure 6 is not as deep as the first. The dynamical theory shows that P/P$_0$ measured in reflection from a periodic diffraction grating at a constant wavelength source such as NIST are expected to be periodic and the amplitude of the oscillations is determined by the beam divergence in φ. On Asterix, the fact that different wavelengths are used to access different spin echo lengths leads to a spin echo signal that is not periodic in y_{se}, i.e. the dips change in amplitude. At large values of y_{se} on Asterix, the spin echo polarization eventually approaches unity because the long wavelength neutrons used can no longer be Bragg reflected by the grating periodicity so only specular reflection is present. In addition, neutrons with large wavelengths cannot penetrate into the grooves of the grating.

5. Acknowledgements

References

[1]   Kim S, Solak H, Stoykovich M , Ferrier N, de Pablo J and Nealey P *2003 Nature* **424** 411-14
[2]   Park S, Lee D, Xu J, Kim B, Hong S, Jeong U, Xu T and Russell T P *2009 Science* **323** 1030-33
[3]   Anastasiadis S H, Russell T P, Satija S K and Majkrzak C F *1989 Phys Rev Lett* **62** 1852-55
[4]   Zhang X, Berry B, Yager K, Kim S, Jones R, Satija S, Pickel D, Douglas J and Karim A *2008 ACS Nano* **2** 2331-41

[5]   Rockford T, Mochrie S G J and Russell T P *2001 Macromolecules* **34** 1487-92

[6]   Berrouane H, André J M, Barchewitz R, Moreno T, Sammar A, Khan Malek C, Pardo B and Rivoira R *1992 Nucl Inst and Meth in Phys Res* A **312** 521-530

[7]   Humphreys C J *1979 Rep Prog Phys* **42** 1825-87

[8]   Ott F, Humbert P, Fermon C and Menelle A *2001 Physica* B **297** 189-93

[9]   Sinha S K, Sirota E B, Garoff S and Stanley H B *1988 Phys Rev* B **38** 2297-311

[10]   Pynn Roger, Fitzsimmons M, Lee W T, Stonaha P, Shah V, Washington A, Kirby B, Majkrzak and Maranville B *2009 Physica* B **404** 2582-84